Research Article

Erik Burman*, Jurriaan J. J. Gillissen and Lauri Oksanen

Stability estimate for scalar image velocimetry

https://doi.org/10.1515/jiip-2020-0107
Received August 15, 2020; revised June 7, 2022; accepted January 26, 2023

Abstract: In this paper, we analyze the stability of the system of partial differential equations modelling scalar image velocimetry. We first revisit a successful numerical technique to reconstruct velocity vectors u from images of a passive scalar field ψ by minimizing a cost functional that penalizes the difference between the reconstructed scalar field ϕ and the measured scalar field ψ, under the constraint that ϕ is advected by the reconstructed velocity field u, which again is governed by the Navier–Stokes equations. We investigate the stability of the reconstruction by applying this method to synthetic scalar fields in two-dimensional turbulence that are generated by numerical simulation. Then we present a mathematical analysis of the nonlinear coupled problem and prove that, in the two-dimensional case, smooth solutions of the Navier–Stokes equations are uniquely determined by the measured scalar field. We also prove a conditional stability estimate showing that the map from the measured scalar field ψ to the reconstructed velocity field u, on any interior subset, is Hölder continuous.

Keywords: Scalar image velocimetry, conditional stability, two-dimensional Navier–Stokes equations, passive transport

MSC 2010: 35R25, 76D05, 35B35, 35Q49, 76M21

1 Introduction

Scalar image velocimetry (SIV) is the reconstruction of the fluid velocity field u from measurements of a scalar field ψ that is advected by u. This idea, which dates back to the works [10, 23, 24], is applied in weather forecasting models using, e.g., satellite images of clouds or ocean temperature. For a background of the technique, see for instance [14] and the references therein.

SIV also finds applications in medical flow imaging and in experimental fluid mechanics. For instance in the laser induced fluorescence (LIF) technique, a fluid is seeded with fluorescent molecules and laser light is focused into a thin sheet, where it is absorbed by the fluorescent molecules followed by spontaneous emission of light which is then recorded by a camera (see, e.g., [21] and the references therein). Assuming that the recorded light intensity is proportional to the fluorescence concentration ψ, the velocity field $u := u_1 e_x + u_2 e_y$, with e_x, e_y being the Cartesian unit vectors, can be reconstructed by invoking the scalar transport equation

$$\partial_t \psi + u \cdot \nabla \psi - \lambda \Delta \psi = 0, \tag{1.1}$$

where λ is the scalar diffusivity. A direct inversion of the scalar transport equation only provides the component $u^\perp$ of u that is normal to ψ isolines:

$$u^\perp = (-\partial_t \psi + \lambda \Delta \psi) \nabla \psi / |\nabla \psi|^2.$$

***Corresponding author: Erik Burman,** Department of Mathematics, University College London, Gower Street, London, WC1E 6BT, United Kingdom, e-mail: e.burman@ucl.ac.uk. https://orcid.org/0000-0003-4287-7241
Jurriaan J. J. Gillissen, Department of Mathematics, University College London, Gower Street, London, WC1E 6BT, United Kingdom, e-mail: jurriaangillissen@gmail.com
Lauri Oksanen, Department of Mathematics and Statistics, University of Helsinki, P.O. 68 (Pietari Kalmin katu 5), 00014 University of Helsinki, Helsinki, Finland, e-mail: lauri.oksanen@helsinki.fi

Finding all components of u requires additional constraints, for example, conservation of hydrodynamic variables.

Inspired by recent developments on computational methods for SIV [13], in this work we study mathematically the stability of the map from ψ to u. We show, in particular, that under suitable a priori assumptions the velocity field is uniquely determined by the measured scalar field, thereby giving a partial theoretical justification to the computational approaches. The analysis uses conditional stability estimates as a workhorse for understanding of inverse problems in a spirit similar to that of the seminal work by Bukhgeĭm and Klibanov [4].

To fix a configuration for the stability analysis, we consider a soap film experiment from [13]. In that work, a soap film with a thickness of $\sim 10\mu$ m is formed in the 10 cm gap between two vertical parallel nylon wires. Turbulence in the film is generated by piercing the film with an array of cylindrical obstacles, resulting in chaotically interacting wake vortices. These perturbations are accompanied by film thickness fluctuations which behave similarly to those of a passive scalar. The soap film is illuminated and light reflections are recorded at high speed. The recorded interference pattern depends on the film thickness fluctuations and therefore behaves similarly to a passive scalar.

Motivated by this experiment, we consider a particular Cartesian geometry $\Omega = (-a, a) \times (-b, b)$, with $a, b > 0$, and write $Q = \Omega \times (0, T)$ for $T > 0$. Our proofs generalize to many other two-dimensional settings, but the above choice allows for convenient notations. We assume that the flow satisfies the slip or no-slip conditions on the vertical boundaries, $x = \pm a$, and that the scalar field satisfies the no-flux condition there, but the boundary conditions for both the velocity u and the scalar field ψ on the top and bottom boundaries $y = \pm b$ are unknown.

Determination of u given ψ is possible only if ψ satisfies some non-degeneracy condition. Indeed, a constant ψ satisfies (1.1) but gives no information on u. To state our main result in a simplified form (see Theorem 4.8 below for the precise formulation), we assume that the spatial derivative of ψ does not vanish identically on the left boundary $x = -a$ at any time.

The simplified formulation is as follows. Let u and $\tilde{u}$ be smooth velocity fields satisfying the Navier–Stokes equations, together with, say, the no-slip boundary condition on $x = \pm a$, and let ψ and $\tilde{\psi}$ be smooth scalar fields satisfying (1.1) with u and $\tilde{u}$, respectively, together with the no-flux boundary condition on $x = \pm a$. Suppose, moreover, that for all $t \in (0, T)$ there is $y \in (-b, b)$ such that $\partial_y \psi(-a, y, t) \neq 0$. Then for every space time domain ω such that $\overline{\omega} \subset Q$ (here and below $\overline{X}$ denotes the closure of the set X), there exist $\alpha \in (0, 1)$ and $C > 0$ such that the following stability estimate holds:

$$\|u - \tilde{u}\|_{L^2(\omega)} \leq C \|\psi - \tilde{\psi}\|^{\alpha}_{H^4(Q)} \tag{1.2}$$

whenever u and $\tilde{u}$ satisfy an a priori bound. Observe that this estimate in particular shows that the scalar field ψ uniquely determines the velocity field u. It also gives an upper bound similar to those applied in [2, 7] to obtain sharp error estimates for finite element data assimilation methods. Although the estimate (1.2) can not be directly applied in that context, it is a first step towards an analysis of the error propagation in computational velocity reconstruction based on SIV.

Our approach combines a stream function formulation for the two-dimensional Navier–Stokes equations, with the classical pressure velocity formulation. First, using a stream function Θ to represent the velocity field u, the convection–diffusion equation for the scalar field ϕ defines a transport equation for Θ. Provided the scalar field satisfies the non-degeneracy condition $\partial_y \psi \neq 0$ on the left boundary, this transport equation can be solved in a neighborhood of the left boundary. This way we show that u can be reconstructed locally given the scalar field ψ. Then to extend this local reconstruction to an arbitrary subdomain in the interior of the space time domain, we apply a unique continuation result for the transient linearized Navier–Stokes equations [16]. Observe that the local reconstruction step is possible whenever the velocity u is known along a curve segment transverse to the level curves of ψ. In our configuration, this holds on the lateral boundaries thanks to the chosen boundary conditions. A variant of this local reconstruction approach, using classical techniques, has recently been applied to SIV in [20].

The outline of this paper is as follows. First, in Section 2, we recall a recent technique for computational velocity reconstruction, and study its stability computationally in Section 3. Then, in Section 4, we prove the conditional stability estimate. This paper ends with concluding remarks in Section 5.

2 An example of a computational method for SIV

In this section, we describe a variational method for the reconstruction of the space and time dependent velocity field u, pressure field p, and scalar field ϕ from a measured space and time dependent scalar field ψ, also referred to as the true scalar field. We assume perfect knowledge of ψ over a space time volume of $\Omega \times (0, T)$, where Ω and $(0, T)$ represent the corresponding spatial and temporal dimensions. The reconstruction method divides $(0, T)$ into segments. Then the i-th segment starts and ends at $t_0 = (i-1)\tau$ and $t_1 = t_0 + \tau$, respectively, where τ is referred to as the segment time. The reconstruction scheme solves a sequence of optimization problems for the unknown state variable $w = (u, p, \phi)$ at the start of each segment, i.e. at $t = t_0$. We use a subscript on a field variable to indicate a time instance, e.g., $w_0 = w(t_0)$. Finding w_0 in each segment involves an iterative scheme, and the initial guess for the iteration is taken from the reconstructed field w_1 at $t = t_1$ obtained in the preceding segment.

2.1 The cost function and its minimization

Defining the state variable by $w = (u, p, \phi)$, the velocity reconstruction method finds the initial conditions for the state variable w_0 in each time segment, by minimizing the deviation between the reconstructed scalar field ϕ and the measured scalar field ψ integrated over $\Omega \times (0, T)$. The corresponding cost functional for the method reads:

$$\mathscr{J} = \frac{1}{2}\int_{t_0}^{t_1} \|\phi - \psi\|^2 \, dt, \tag{2.1}$$

where the norm $\|\cdot\|$ is based on the $L^2(\Omega)$ inner product, denoted by $\langle \cdot, \cdot \rangle$.

Equation (2.1) is minimized under the constraint that w_1 is related to w_0 via the conservation equations of fluid momentum, fluid mass, and scalar field:

$$R(w) = \begin{pmatrix} \partial_t u + u \cdot \nabla u + \nabla p - \nu \Delta u \\ \nabla \cdot u \\ \partial_t \phi + u \cdot \nabla \phi - \lambda \Delta \phi \end{pmatrix} = 0. \tag{2.2}$$

Here ν is the fluid kinematic viscosity and λ is the scalar diffusivity. Adding constraint (2.2) to equation (2.1) using the Lagrange multiplier $\hat{w} = (\hat{u}, \hat{p}, \hat{\phi})$ results in the following constrained cost functional, which is referred to as the Lagrangian $\mathscr{L}$:

$$\mathscr{L} = \int_{t_0}^{t_1} \Big(\frac{1}{2}\|\phi - \psi\|^2 + \langle \hat{w}, R(w) \rangle \Big) \, dt. \tag{2.3}$$

Minimizing $\mathscr{L}$ of (2.3) with respect to w_0 involves computing the gradient of $\mathscr{L}$ with respect to w_0, i.e. $\delta\mathscr{L}/\delta w_0$. Following [13], we obtain

$$\frac{\delta \mathscr{L}}{\delta w_0} = \begin{pmatrix} \frac{\delta \mathscr{L}}{\delta u_0} \\ \frac{\delta \mathscr{L}}{\delta p_0} \\ \frac{\delta \mathscr{L}}{\delta \phi_0} \end{pmatrix} = \begin{pmatrix} -\hat{u}_0 \\ 0 \\ -\hat{\phi}_0 \end{pmatrix}. \tag{2.4}$$

This expression for $\delta\mathscr{L}/\delta w_0$ contains the Lagrange multiplier $\hat{w} = (\hat{u}, \hat{p}, \hat{\phi})$, whose evolution equation and initial and final conditions read:

$$\begin{pmatrix} -\partial_t \hat{u} - u \cdot (\nabla \hat{u} + \nabla \hat{u}^T) - \nabla \hat{p} - \nu \Delta \hat{u} - \phi \nabla \hat{\phi} \\ -\nabla \cdot \hat{u} \\ -\partial_t \hat{\phi} - u \cdot \nabla \hat{\phi} - \lambda \Delta \hat{\phi} + \phi - \psi \end{pmatrix} = 0, \tag{2.5a}$$

$$\hat{u}_1 = 0, \quad \hat{\phi}_1 = 0, \tag{2.5b}$$

$$\hat{u}_0 = 0, \quad \hat{\phi}_0 = 0. \tag{2.5c}$$

Equation (2.5a) governs the evolution of the Lagrange multiplier $\hat{w} = (\hat{u}, \hat{p}, \hat{\phi})$, showing that $\hat{u}$ is incompressible and is forced along gradients of $\hat{\phi}$, and that both $\hat{u}$ and $\hat{\phi}$ are advected by u and are subjected to diffusion.

The diffusion coefficients $-\nu$ and $-\lambda$ of these transport equations are negative, and therefore these equations are integrated backward in time from $t = t_1$ to $t = t_0$. The 'starting' conditions $\hat{w}_1$ at $t = t_1$ are given by equation (2.5b), while the 'final' conditions $\hat{w}_0$ at $t = t_0$ define the optimization update direction of w_0 via (2.4). This direction approaches zero when w_0 reaches an extremum of $\mathscr{L}$, which corresponds to the condition of (2.5c).

To find w_0, we use the Polak–Rebiere variant of the conjugate gradient method [18], which updates w_0 along a search direction h related to $\delta\mathscr{L}/\delta w_0$. The initial guess for w_0 is w_1 from the previous time segment, and the step length along h is varied using Brent's line minimization algorithm [3], until the minimum of the functional $\mathscr{J}$, from (2.1), in this direction is found. The conjugate gradient algorithm is continued until the relative change in $\mathscr{J}$ between two consecutive iterations drops below 0.01. A reconstruction typically require $\sim 10^2$ conjugate gradient steps and ~ 10 Brent minimization steps per conjugate gradient step. Therefore the computational effort of both methods is equivalent to that of $\sim 10^3$ computational fluid dynamics simulations.

It was shown in [13] that the reconstruction method produces unstable results when the segment time τ is larger than the flow correlation time $\mathscr{T}$, which for the system described above corresponds to $\tau \gtrsim 0.1$. The instability is related to the ill-posedness of the initial value problem for chaotic systems, which corresponds to the cost functional developing multiple minima, when τ exceeds $\mathscr{T}$; see, for instance, [17]. In order to stabilize the method for these cases, regularization terms may be added to the functional of (2.1). In this work, we restrict ourselves to $\tau \lesssim 0.1$, which does not require the use of these regularization terms.

3 Numerical investigation of the stability of SIV

3.1 Setup

We apply the computational velocity reconstruction to a two-dimensional, incompressible, decaying turbulent flow field in a space time domain $\Omega \times (0, T)$. The spatial domain $\Omega = (-\pi, \pi)^2$ is a bi-periodic square with side length $L = 2\pi$ and the temporal domain $(0, T)$ has a size of $T = 8$, which is referred to as the reconstruction time. The objective is to reconstruct the velocity field u from the measured space and time dependent scalar field ψ. To distinguish between the reconstructed velocity field and the reference velocity field, giving the advection of ψ, we denote the former by u and the latter by v. It is re-emphasized that we have access to perfect information of ψ on $\Omega \times (0, T)$.

Both ψ and v start from random initial conditions and the initial conditions are normalized such that $\mathscr{U} = \|v\| = 1$ and $\|\psi\| = 1$ at $t = 0$. The diffusivity is $\lambda = 2 \times 10^{-3}$ and the viscosity is $\nu = 1 \times 10^{-3}$, which corresponds to a Reynolds number of $\mathrm{Re} = \mathscr{U}L/\nu = 6.3 \times 10^3$ based on the initial velocity scale $\mathscr{U}$ and a Schmidt number of $\mathrm{Sc} = \nu/\lambda = \frac{1}{2}$. We furthermore use a segment time of $\tau = 8 \times 10^{-2}$.

The true velocity field v and the true (measured) scalar field ψ are generated on a 256^2 grid by numerically integrating (2.2). Subsequently, the scalar measurement is interpolated to a 128^2 grid and the reconstruction fields u and ϕ are obtained on this 128^2 grid by iteratively integrating equations (2.2), (2.4) and (2.5). On both the 256^2 and 128^2 grids, equations (2.2) and (2.5a) are advanced in time using a computational time step of $\Delta t = 10^{-3}$. Spatial derivatives in these equations are computed using the Fourier basis functions. Time integration is performed using the second-order explicit Adams–Bashforth scheme for the advection terms and the second-order implicit Crank–Nicolson scheme for the diffusion terms. For further details on the numerical methods, see [11–13].

3.2 Results

Figure 1a shows the reconstruction error $\epsilon = \|u - v\|^2$ as a function of time, where it is recalled that u is the reconstructed velocity and v is the reference velocity field. It is seen that, with time, ϵ first decreases and after $t > 4$, the error levels off.

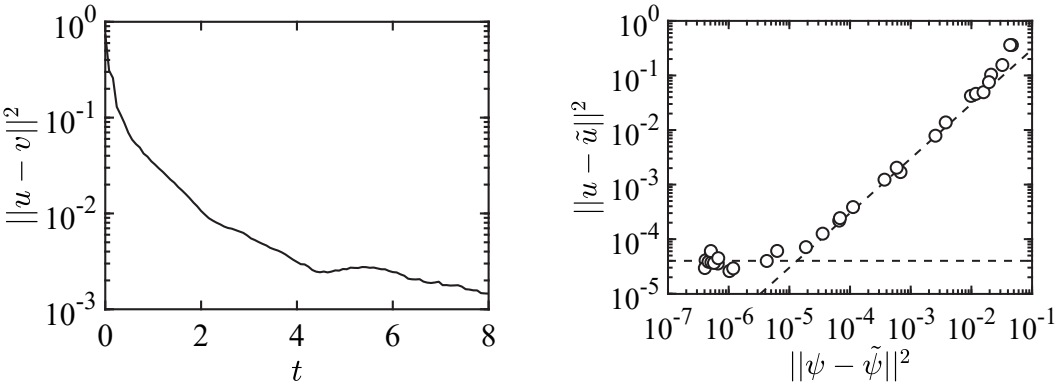

(a) Reconstruction error versus time.

(b) Variation in reconstructed velocity versus variation in measured scalar.

Figure 1: Reconstruction error and variation in reconstructed velocity.

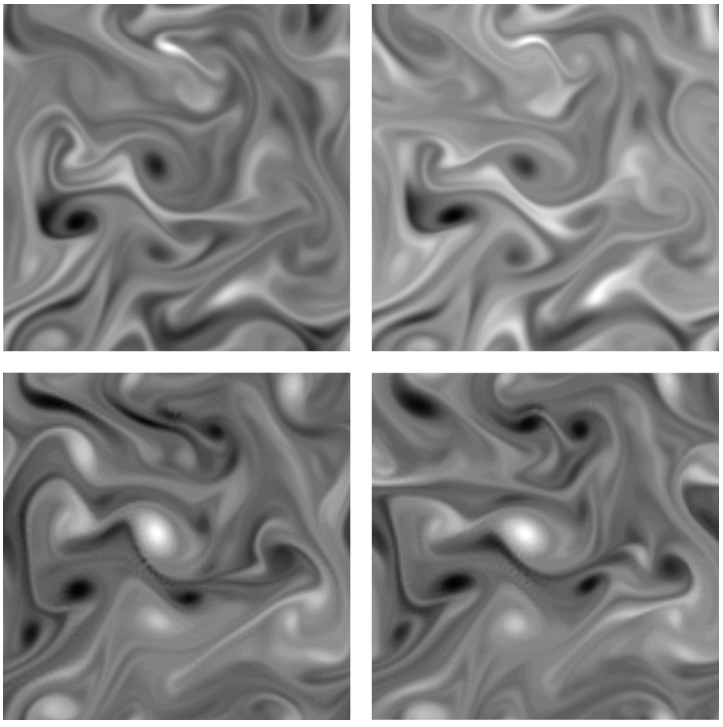

Figure 2: (Top) Two 'measured' scalar fields, ψ and $\tilde{\psi}$, at $t = 6$, that are advected by two 'true' velocity fields v and $\tilde{v}$. At $t = 0$ it was assumed that $\tilde{\psi} = \psi$ and that $\tilde{v} = v + \delta v$ where $\|\delta v\|/\|v\| = 10^{-1}$. (Bottom) The curl of the corresponding reconstructed velocity fields, u and $\tilde{u}$, at $t = 6$.

Recalling the time segmentation described in the first paragraph in Section 2, the time dependent behavior in Figure 1a indicates that the reconstruction depends on the quality of the initial guess for the initial condition at the start of each segment. In the first segment, the initial guess is zero, while in each consecutive segment the initial guess becomes closer to the reference solution, explaining the observed decrease in ϵ with time. Also, recall that the stability of the unique continuation problem for parabolic equations degenerates towards $t = 0$, so a similar effect is expected also for globally coupled solutions.

We now study the convergence of the reconstructed u as a function of the true (measured) ψ. To this end, we generate multiple simulations of true scalar fields ψ that are advected by different 'true' velocity fields v. For these simulations, the conditions at $t = 0$ for ψ are identical but the conditions for v differ. Differences in a quantity q between two simulations are denoted by $q - \tilde{q}$. The relative difference in the initial conditions is

varied between 10^{-5} and 10^{-1}. To study the convergence of u as a function of ψ, we plot $\|u - \tilde{u}\|^2$ as a function of $\|\psi - \tilde{\psi}\|^2$ in Figure 1b. It is noted that we average this norm over a time interval of $6 < t < 8$. During this time interval, the computational method has converged roughly to a steady state, as shown in Figure 1a.

Figure 1b shows that there are two regimes in the dependence of the variation of the reconstructed velocity $\|u - \tilde{u}\|^2$ on the variation of the true scalar $\|\psi - \tilde{\psi}\|^2$:

$$\|u - \tilde{u}\|^2 \sim \begin{cases} \text{constant} & \text{for } \|\psi - \tilde{\psi}\|^2 \lesssim 10^{-5}, \\ \|\psi - \tilde{\psi}\|^2 & \text{for } \|\psi - \tilde{\psi}\|^2 \gtrsim 10^{-5}. \end{cases} \tag{3.1}$$

These regimes are indicated by the dashed lines in Figure 1b which have a slope of zero and one, respectively. In these regimes, the variation of the true scalar $\|\psi - \tilde{\psi}\|^2$ (and of the true velocity $\|v - \tilde{v}\|^2$) is smaller and larger, respectively, than the error of the reconstructed velocity $\|u - v\|^2$. Consequently, the variation of the reconstructed velocity $\|u - \tilde{u}\|^2$ in these two regimes is set by $\|u - v\|^2$ (constant) and by $\|\psi - \tilde{\psi}\|^2$, respectively. The level of stagnation depends on the time and space resolution of the Navier–Stokes solver, which limits the accuracy of the reconstructed velocity. The second regime of (3.1) corresponds to Lipschitz stability of the velocities. In view of the classical stability result [8] for data assimilation problems subject to the heat equation, Lipschitz stability is feasible thanks to the fact that only the initial data of u are unknown in this computational example. We also show that the local reconstruction step is Lipschitz stable; see Remark 4.6 below. We leave a precise numerical analysis of the computational error as a topic of a future work; see [7] for such an analysis of data assimilation problems subject to the heat equation.

For illustration purposes, we show in Figure 2 (top) two true scalar fields, ψ and $\tilde{\psi}$, at $t = 6$, that are advected by two 'true' velocity fields v and $\tilde{v}$. At $t = 0$ it was assumed that $\tilde{\psi} = \psi$ and that $\tilde{v} = v + \Delta v$ where $\|\Delta v\|/\|v\| = 10^{-1}$. Figure 2 (bottom) shows the curl of the corresponding reconstructed velocity fields, u and $\tilde{u}$, at $t = 6$.

4 Stability analysis

In this section, we will derive a stability estimate that gives a mathematical interpretation of the stability illustrated by the right plot of Figure 1. Compared to the numerical example, we consider a more challenging setting where not only the initial data but also the boundary data on parts of the boundary are unknown. While the stability estimate shows that convergence as in Figure 1 is possible to obtain, it does not imply that the method in Section 2.1 must converge.

To fix the ideas, we consider a simplified geometric configuration similar to that of a two-dimensional soap film experiment described above. Let $\Omega = (-a, a) \times (-b, b)$ and write $Q = \Omega \times (0, T)$. The vertical boundaries of the domain are defined by

$$\Sigma = \Sigma_- \cup \Sigma_+, \quad \Sigma_\pm = \{(x, y) : x = \pm a \text{ and } y \in (-b, b)\}.$$

Let u be a solution to the Navier–Stokes equations in Q:

$$\begin{cases} \partial_t u - \nu \Delta u + (u \cdot \nabla) u + \nabla p = 0, \\ \nabla \cdot u = 0. \end{cases} \tag{4.1}$$

On Σ we assume that u satisfies either homogeneous Dirichlet conditions

$$u = 0, \tag{4.2}$$

or slip conditions, i.e.

$$u \cdot n = 0, \tag{4.3}$$

where n is the outward pointing normal on Σ. On the top and bottom boundaries, the boundary data are unknown. The viscosity coefficient $\nu > 0$ is known.

We suppose that a passive scalar ψ satisfies

$$\partial_t \psi + u \cdot \nabla \psi - \lambda \Delta \psi = 0 \tag{4.4}$$

in Q, together with the no-flux boundary condition

$$u_1 \psi - \lambda \partial_x \psi = 0 \quad \text{on } \Sigma. \tag{4.5}$$

Observe that the Dirichlet and slip conditions imply that the first component of u vanishes on Σ, that is, this reduces to a Neumann condition in practice. The diffusivity coefficient $\lambda > 0$ is a known constant.

Recall that the inverse problem to find u given ψ is clearly unsolvable if ψ is a constant function, so we make the standing assumption that this is not the case. More precisely, we will assume that ψ is non-constant in space on Σ.

It is well-known that the Navier–Stokes equations admit smooth solutions in the two-dimensional case; see, e.g., [22, Remark 3.7, p. 303]. For simplicity, we assume that both u and ψ are smooth in $\overline{\Omega} \times (0, T)$.

Note that smoothness of ψ in the interior of Q actually follows from the interior Schauder estimates for (4.4) and smoothness of u; see, e.g., [15, Theorem 8.12.1, p. 131]. However, as we do not assume any boundary conditions on the horizontal boundaries $y = \pm b$, we do not enter into discussion of smoothness properties of ψ.

4.1 Stream function

As Ω is a two-dimensional simply connected domain, the vanishing of the divergence $\nabla \cdot u = 0$ implies that there is Θ such that

$$u = (\partial_y \Theta, -\partial_x \Theta). \tag{4.6}$$

Observe that (4.4) implies

$$\partial_y \Theta \partial_x \psi - \partial_x \Theta \partial_y \psi = \zeta,$$

where $\zeta = \zeta_\psi = -\partial_t \psi + \lambda \Delta \psi$. Defining the (time-dependent) vector field

$$X = X_\psi = -\partial_y \psi \partial_x + \partial_x \psi \partial_y \tag{4.7}$$

on Ω, we can write equivalently

$$X\Theta = \zeta, \tag{4.8}$$

viewing the vector field X as the differential operator defined by (4.7).

As $\partial_y \Theta = u_1 = 0$ on Σ, due to the boundary condition on u, and as the stream functions Θ and $\Theta + c$, with $c \in \mathbb{R}$ being a constant, give the same u, we may assume that

$$\Theta|_{\Sigma_-} = 0. \tag{4.9}$$

We can view (4.8)–(4.9) as a transport equation for Θ. Observe that the vector field X and the right-hand side ζ are known as ψ is known.

Suppose that $\partial_y \psi(p_0) \neq 0$ for a point $p_0 \in \Sigma_- \times (0, T)$. Then, near p_0, we can rewrite (4.8) as

$$\partial_x \Theta + \beta \partial_y \Theta = f, \tag{4.10}$$

where $\beta = -(\partial_y \psi)^{-1} (\partial_x \psi)$ and $f = (\partial_y \psi)^{-1} \zeta$. Together with the boundary condition (4.9), this transport equation can be solved near p_0. In particular, recalling (4.6), we see that ψ determines u near p_0. We will next study the continuity of the map $\psi \mapsto u$ near p_0. Observe that this map is nonlinear, both β and f depend on ψ.

4.2 On stability of linear transport equations

In this section, we study linear transport equations in an abstract setting, and the meaning of the variables here are different from those above.

Consider the equation

$$\partial_t u + \beta \cdot \nabla u = f \tag{4.11}$$

with the initial condition $u|_{t=0} = 0$. We are interested in the continuity properties of the map $(f, \beta) \mapsto u$. However, let us first recall the standard continuity result for the map $f \mapsto u$ with β fixed. The exposition below was inspired by [9, Theorem 7, p. 131] where more complicated Hamilton–Jacobi equations are considered. Contrary to this reference, we need to keep track of the dependence on β of the constants in the estimates.

Let $T > 0$, suppose that $\beta \in L^\infty(0, T; W^{1,\infty}(\mathbb{R}^n; \mathbb{R}^n))$, and choose

$$R \geq \|\beta\|_{L^\infty((0,T)\times\mathbb{R}^n;\mathbb{R}^n)}.$$

Furthermore, define $r(t) = R(T - t)$, let $B(r) \subset \mathbb{R}^n$ be the open ball of radius r, with a fixed center and outward pointing normal n_B, and consider the energy

$$E(t) = \int_{B(r(t))} u^2(t, x)\, dx.$$

Then for a solution u of (4.11),

$$\partial_t E \leq CE + \int_{B(r)} f^2\, dx, \tag{4.12}$$

where

$$C = 1 + \|\beta\|_{L^\infty(0,T;W^{1,\infty}(\mathbb{R}^n;\mathbb{R}^n))}.$$

Indeed, using

$$\partial_t u^2 = 2u\partial_t u = -2u\beta \cdot \nabla u + 2uf = 2uf - \beta \cdot \nabla u^2,$$

we get

$$\begin{aligned}
\partial_t E &= \int_{B(r)} 2u\partial_t u\, dx + r' \int_{\partial B(r)} u^2\, dx \\
&= \int_{B(r)} 2uf - \beta \cdot \nabla u^2\, dx + r' \int_{\partial B(r)} u^2\, dx \\
&= \int_{B(r)} 2uf + u^2 \nabla \cdot \beta\, dx - \int_{\partial B(r)} u^2 n_B \cdot \beta\, dx + r' \int_{\partial B(r)} u^2\, dx \\
&\leq \int_{B(r)} 2uf + u^2 \nabla \cdot \beta\, dx,
\end{aligned}$$

where we used $|n_B \cdot \beta| \leq R = -r'$.

Now (4.12) follows from the Cauchy–Schwarz inequality. We write

$$\mathcal{C} = \{t \in (0, T) : x \in B(r(t))\}.$$

Grönwall's inequality implies the following lemma.

Lemma 4.1. *Let $\beta \in L^\infty(0, T; W^{1,\infty}(\mathbb{R}^n; \mathbb{R}^n))$. Then there is $C > 0$ such that*

$$\|u(t)\|_{L^2(B(r(t)))} \leq C\|f\|_{L^2(\mathcal{C})}, \quad t \in (0, T),$$

for all $u \in C^1(\overline{\mathcal{C}})$ satisfying (4.11) *and $u|_{t=0} = 0$. The constant C depends only on T and the norm of β.*

We need also higher order energy estimates. For notational simplicity, let us now consider only the case $n = 1$. Let $k \in \mathbb{N}$. If u satisfies (4.11), then $v = \partial_x^k u$ satisfies

$$\partial_t v + \beta \partial_x v = \tilde{f}, \quad \tilde{f} = \partial_x^k f - [\partial_x^k, \beta\partial_x]u.$$

We write

$$\tilde{E}_k = \int_{B(r)} v^2\, dx, \quad E_K = \sum_{k=0}^{K} \int_{B(r)} (\partial_x^k u)^2\, dx.$$

Applying (4.12) to v gives

$$\partial_t \tilde{E}_k \le C\tilde{E}_k + \int_{B(r)} \tilde{f}^2\,dx \le C\tilde{E}_k + \int_{B(r)} (\partial_x^k f)^2\,dx + C\tilde{E}_k, \tag{4.13}$$

where the constant depends only on the $L^\infty(0,T;W^{k,\infty}(\mathbb{R}))$-norm of β. The sum of the estimates (4.13) for $k = 0,\dots,K$ gives

$$\partial_t E_K \le CE_K + C\sum_{k=0}^{K}\int_{B(r)} (\partial_x^k f)^2\,dx. \tag{4.14}$$

Grönwall's inequality gives the following lemma.

Lemma 4.2. *Let $k \ge 1$ and $\beta \in L^\infty(0,T;W^{k,\infty}(\mathbb{R}))$. Then there is $C > 0$ such that*

$$\|u(t)\|_{H^k(B(r(t)))} \le C\sum_{j=0}^{k}\|\partial_x^k f\|_{L^2(\mathcal{C})}, \quad t \in (0,T),$$

for all $u \in C^{k+1}(\overline{\mathcal{C}})$ satisfying (4.11) *and $u|_{t=0} = 0$. The constant C depends only on T and the norm of β.*

We can apply a similar argument also to the time derivative. We will need only the first derivative in time $v = \partial_t u$. Then

$$\partial_t v + \beta\partial_x v = \tilde{f}, \quad \tilde{f} = \partial_t f - (\partial_t\beta)\partial_x u.$$

Writing $\tilde{E} = \int_{B(r)} v^2\,dx$ and applying (4.12) to v gives

$$\partial_t \tilde{E} \le C\tilde{E} + C\int_{B(r)} \tilde{f}^2\,dx \le C\tilde{E} + \int_{B(r)} (\partial_t f)^2\,dx + CE_1,$$

where the constant depends only on the $W^{1,\infty}((0,T)\times\mathbb{R})$-norm of β. The sum of this and (4.14) with $K = 1$, together with Grönwall's inequality, gives the following lemma.

Lemma 4.3. *Let $\beta \in W^{1,\infty}((0,T)\times\mathbb{R})$. Then there is $C > 0$ such that*

$$\|\partial_t u(t)\|_{L^2(B(r(t)))} + \|u(t)\|_{H^1(B(r(t)))} \le C\|f\|_{H^1(\mathcal{C})}, \quad t \in (0,T),$$

for all $u \in C^2(\overline{\mathcal{C}})$ satisfying (4.11) *and $u|_{t=0} = 0$. The constant C depends only on T and the norm of β.*

Corollary 4.4. *Let $\beta_1, \beta_2 \in W^{1,\infty}((0,T)\times\mathbb{R})$ and suppose that*

$$\|\beta_j\|_{L^\infty((0,T)\times\mathbb{R})} \le R, \quad \|\beta_j\|_{W^{1,\infty}((0,T)\times\mathbb{R})} \le R_1.$$

Let $u_j \in C^2(\overline{\mathcal{C}})$ satisfy $u_j|_{t=0} = 0$ and $\partial_t u_j + \beta_j\partial_x u_j = f_j$, $j = 1,2$. Suppose furthermore that $\|f_j\|_{H^1(\mathcal{C})} \le R_1$. Then

$$\|u_1 - u_2\|_{H^1(\mathcal{C})} \le C(\|f_1 - f_2\|_{H^1(\mathcal{C})} + \|\beta_1 - \beta_2\|_{W^{1,\infty}(\mathcal{C})}),$$

where the constant depends only on T and R_1.

Proof. The function $w = u_1 - u_2$ satisfies

$$\partial_t w + \beta_1\partial_x w = f_1 - f_2 + (\beta_2 - \beta_1)\partial_x u_2,$$

and from Lemma 4.3 we have

$$\|w\|_{H^1(\mathcal{C})} \le C\|f_1 - f_2\|_{H^1(\mathcal{C})} + C\|\beta_1 - \beta_2\|_{W^{1,\infty}(\mathcal{C})}\|u_2\|_{H^1(\mathcal{C})}.$$

Using $\|f_2\|_{H^1(\mathcal{C})} \le R_1$, the claim follows from Lemma 4.3. □

4.3 Local recovery

We will now apply Corollary 4.4 to (4.10).

Proposition 4.5. *Let $\psi \in H^4(Q)$ and suppose that $\partial_y\psi(p_0) \ne 0$ for a point p_0 in $\Sigma_- \times (0,T)$. Let $U_0 \subset \overline{\Omega}\times(0,T)$ be a neighborhood of p_0. Then there are a neighborhood $\mathcal{B} \subset H^4(Q)$ of ψ, a neighborhood $U \subset U_0$ of p_0 and a constant*

$C > 0$ such that for all $\tilde{\psi} \in \mathcal{B}$ there holds

$$\|\Theta - \tilde{\Theta}\|_{H^1(U)} \leq C\|\psi - \tilde{\psi}\|_{H^4(U)},$$

where Θ and $\tilde{\Theta}$ are the solutions of (4.8)–(4.9) *with $(X, \zeta) = (X_\psi, \zeta_\psi)$ and $(X, \zeta) = (X_{\tilde{\psi}}, \zeta_{\tilde{\psi}})$, respectively.*

Proof. The Sobolev embedding theorem implies that $\psi \in C^2(\overline{Q})$. In particular, the point value $\partial_y\psi(p_0)$ is well-defined and there are a neighborhood V of p_0 and $\epsilon > 0$ such that $|\partial_y\psi(p)| > \epsilon$ for all $p \in V$. Define $\beta = -(\partial_y\psi)^{-1}(\partial_x\psi)$ in V, cf. (4.10), and

$$R = 1 + \|\beta\|_{L^\infty(V)}.$$

Write $p_0 = (-a, y_0, t_0)$ and consider the set

$$U = \{(x, y, t) \in Q : x \in (-a, -a + \delta),\ |y - y_0| < R(\delta - (x + a)),\ |t - t_0| < \delta\},$$

where $\delta > 0$ is small enough so that $\overline{U} \subset V \cap U_0$. Choose a small enough neighborhood $\mathcal{B} \subset H^4(Q)$ of ψ so that $\tilde{\beta} = -(\partial_y\tilde{\psi})^{-1}(\partial_x\tilde{\psi})$ satisfies $\|\tilde{\beta}\|_{L^\infty(V)} \leq R$ for all $\tilde{\psi} \in \mathcal{B}$. Now Corollary 4.4 implies the claimed estimate. Indeed,

$$\|\beta - \tilde{\beta}\|_{W^{1,\infty}(U)} \leq C\|\psi - \tilde{\psi}\|_{W^{2,\infty}(U)} \leq C\|\psi - \tilde{\psi}\|_{H^4(U)}.$$

Writing $f = (\partial_y\psi)^{-1}\zeta$, with $\zeta = -\partial_t\psi + \lambda\Delta\psi$, and defining $\tilde{f}$ analogously, we obtain

$$\|f - \tilde{f}\|_{H^1(U)} \leq C\|\psi - \tilde{\psi}\|_{W^{2,\infty}(U)} + C\|\psi - \tilde{\psi}\|_{H^3(U)}.$$

Here the constants depend on

$$\sup_{\tilde{\psi}\in\mathcal{B}}\|\tilde{\psi}\|_{H^4(Q)} \quad \text{and} \quad \Big(\inf_{\tilde{\psi}\in\mathcal{B}, p\in V}|\partial_y\tilde{\psi}(p)|\Big)^{-1}. \qquad \square$$

Remark 4.6. Using notation from the above proposition, it is immediate from equation (4.6) that

$$\|u - \tilde{u}\|_{L^2(U)} \leq \|\Theta - \tilde{\Theta}\|_{H^1(U)} \leq C\|\psi - \tilde{\psi}\|_{H^4(U)}, \quad \tilde{\phi} \in \mathcal{B},$$

where (ϕ, u) and $(\tilde{\phi}, \tilde{u})$ both satisfy (1.1) together with the boundary conditions (4.5) and $u_1 = 0$ on Σ. Hence the map $\psi \mapsto u$ is locally Lipschitz continuous.

4.4 Global recovery

We recall the three cylinders inequality for the linearized Navier–Stokes equation from [16]; see also [1] for an earlier related result. Let $u \in H^1(0, T; H^2_{loc}(\Omega))$ be a nontrivial solution of (4.1) with associated pressure $p \in L^2(0, T; H^1(\Omega))$. Let $B(x, R) \subset \mathbb{R}^2$ denote the ball of radius R with the center x.

Theorem 4.7 ([16]). *Let $C_0, T > 0$, $0 < R_1 < R_2 < R_3/3 < 1$, $x_0 \in \Omega$, and let $\epsilon > 0$ be small. Suppose $B(x_0, R_3) \subset \Omega$. Then there are $C > 0$ and $\alpha \in (0, 1)$ such that*

$$\int_\epsilon^{T-\epsilon}\int_{B(x_0,R_2)}|u|^2\,dx\,dt \leq C\Big(\int_0^T\int_{B(x_0,R_1)}|u|^2\,dx\,dt\Big)^\alpha\Big(\int_0^T\int_{B(x_0,R_3)}|u|^2\,dx\,dt\Big)^{1-\alpha}$$

for all solutions to

$$\begin{cases}\partial_t u - \nu\Delta u + (A\cdot\nabla)u + (u\cdot\nabla)B + \nabla p = 0,\\ \nabla\cdot u = 0,\end{cases} \tag{4.15}$$

in Q and all $A, B \in L^\infty(Q)$ satisfying $\|A\|_{L^\infty(Q)} \leq C_0$ and $\|B\|_{L^\infty(Q)} \leq C_0$.

This together with the local recovery implies the following global recovery. Recall that both for Dirichlet and slip conditions, i.e. (4.2) and (4.3), we have $u_1 = 0$ on Σ.

Theorem 4.8. *Let $U \subset \mathbb{R}^2$ be open and suppose that $\overline{U} \subset \Omega$. Let $C_0 > 0$, $t_0 \in (0, T)$, and $y_0 \in (-b, b)$. Define*

$$\mathcal{U} = \{u \in C^\infty(Q) : u \text{ satisfies (4.1)}, \ u_1 = 0 \text{ on } \Sigma, \text{ and } \|u\|_{L^\infty(Q)} \le C_0\}.$$

Let $u \in \mathcal{U}$ and let $\psi \in H^4(Q)$ satisfy (4.4)–(4.5) and $\partial_y \psi(p_0) \neq 0$, where $p_0 = (-a, y_0, t_0)$. Let $U_0 \subset \overline{\Omega} \times (0, T)$ be a neighborhood of p_0. Then there are a neighborhood $\mathcal{B} \subset H^4(Q)$ of ψ and constants $\alpha \in (0, 1)$ and $C, s > 0$ such that if $\tilde{u} \in \mathcal{U}$ and if $\tilde{\psi} \in \mathcal{B}$ satisfies (4.4)–(4.5), with u replaced by $\tilde{u}$, then

$$\|u - \tilde{u}\|_{L^2((t_0-s,t_0+s)\times U)} \le C\|\psi - \tilde{\psi}\|^\alpha_{H^4(U_0)}.$$

Proof. Proposition 4.5 implies that there are a neighborhood $\mathcal{B} \subset H^4(Q)$ of ψ and a neighborhood $U_1 \subset U_0$ of p_0 such that

$$\|u - \tilde{u}\|_{L^2(U_1)} \le C\|\psi - \tilde{\psi}\|_{H^4(U_1)}, \quad \tilde{\psi} \in \mathcal{B}.$$

The difference $e = u - \tilde{u}$ satisfies (4.15) with $A = u$ and $B = \tilde{u}$. Indeed,

$$(A \cdot \nabla)e + (e \cdot \nabla)B = (u \cdot \nabla)(u - \tilde{u}) + ((u - \tilde{u}) \cdot \nabla)\tilde{u} = (u \cdot \nabla)u - (\tilde{u} \cdot \nabla)\tilde{u}.$$

We can then apply Theorem 4.7 to e. Taking $B(x_0, R_1) \subset U_1$, it follows that for $R_2 > 0$ as in Theorem 4.7 there holds

$$\int_\epsilon^{T-\epsilon} \int_{B(x,R_2)} |e|^2 \, dx \, dt \le C(\|\psi - \tilde{\psi}\|^2_{H^4(U_0)})^\alpha (\|u\|^2_{L^2(Q)} + \|\tilde{u}\|^2_{L^2(Q)})^{1-\alpha}.$$

The claim follows by iterating Theorem 4.7 finitely many times (see for instance [19]). □

5 Concluding remarks

We have shown that, for the SIV problem, the velocity field u is uniquely determined by the measured scalar field ψ, and u depends continuously on ψ. The stability is of Hölder type for the interior estimates considered here. Due to the nonlinearity of the map $\psi \mapsto u$, the scalar field in the right-hand side of the stability estimate of Theorem 4.8 is measured in the H^4-norm. This is much stronger than the L^2-norm of the velocities in the left-hand side, but it seems unlikely that it can be improved by much in the framework exposed here. The consequence of this lack of balance in the estimate is that computationally we must expect the error in the velocity to be larger than that in the scalar field, even if $\alpha \approx 1$.

An outstanding challenge is to further develop the analysis so that it allows for error estimates for a computational method. Several building blocks for such a development are available, for convection–diffusion equations and transport in [5, 6], for parabolic problems in [7] and for the stationary linearized Navier–Stokes equation in [2]. In those references, finite element methods are considered, but the arguments can be reinterpreted in the context of spectral or Fourier methods that we considered here.

Funding: The first author was supported by EPSRC grants EP/T033126/1 and EP/P01576X/1. The second author was supported by the EPSRC grant EP/N024915/1. The third author was supported by EPSRC grants EP/L026473/1 and EP/P01593X/1.

References

[1] M. Bellassoued, O. Imanuvilov and M. Yamamoto, Carleman estimate for the Navier-Stokes equations and an application to a lateral Cauchy problem, *Inverse Problems* **32** (2016), no. 2, Article ID 025001.

[2] M. Boulakia, E. Burman, M. A. Fernández and C. Voisembert, Data assimilation finite element method for the linearized Navier–Stokes equations in the low Reynolds regime, *Inverse Problems* **36** (2020), no. 8, Article ID 085003.

[3] R. P. Brent, *Algorithms for Minimization Without Derivatives*, Courier Corporation, New York, 2013.

[4] A. L. Bukhgeĭm and M. V. Klibanov, Uniqueness in the large of a class of multidimensional inverse problems, *Dokl. Akad. Nauk SSSR* **260** (1981), no. 2, 269–272.
[5] E. Burman, M. Nechita and L. Oksanen, A stabilized finite element method for inverse problems subject to the convection-diffusion equation. I: Diffusion-dominated regime, *Numer. Math.* **144** (2020), no. 3, 451–477.
[6] E. Burman, M. Nechita and L. Oksanen, A stabilized finite element method for inverse problems subject to the convection-diffusion equation. II: convection-dominated regime, *Numer. Math.* **150** (2022), no. 3, 769–801.
[7] E. Burman and L. Oksanen, Data assimilation for the heat equation using stabilized finite element methods, *Numer. Math.* **139** (2018), no. 3, 505–528.
[8] O. Y. Èmanuilov, Controllability of parabolic equations, *Mat. Sb.* **186** (1995), no. 6, 109–132.
[9] L. C. Evans, *Partial Differential Equations*, 2nd ed., Grad. Stud. Math. 19, American Mathematical Society, Providence, 2010.
[10] M. E. Fiadeiro and G. Veronis, Obtaining velocities from tracer distributions, *J. Phys. Oceanography* **14** (1984), no. 11, 1734–1746.
[11] J. J. J. Gillissen, Two-dimensional decaying elastoinertial turbulence, *Phys. Rev. Lett.* **123** (2019), no. 14, Article ID 144502.
[12] J. J. J. Gillissen, R. Bouffanais and D. K. P. Yue, Data assimilation method to de-noise and de-filter particle image velocimetry data, *J. Fluid Mech.* **877** (2019), 196–213.
[13] J. J. J. Gillissen, A. Vilquin, H. Kellay, R. Bouffanais and D. K. P. Yue, A space-time integral minimisation method for the reconstruction of velocity fields from measured scalar fields, *J. Fluid Mech.* **854** (2018), 348–366.
[14] E. Kalnay, *Atmospheric Modeling, Data Assimilation and Predictability*, Cambridge University, Cambridge, 2003.
[15] N. V. Krylov, *Lectures on Elliptic and Parabolic Equations in Hölder Spaces*, Grad. Stud. Math. 12, American Mathematical Society, Providence, 1996.
[16] C.-L. Lin and J.-N. Wang, Quantitative uniqueness estimates for the generalized non-stationary Stokes system, *Appl. Anal.* **101** (2022), no. 10, 3591–3611.
[17] C. Pires, R. Vautard and O. Talagrand, On extending the limits of variational assimilation in nonlinear chaotic systems, *Tellus A* **48** (1996), no. 1, 96–121.
[18] E. Polak, *Computational Methods in Optimization. A Unified Approach*, Math. Sci. Eng. 77, Academic Press, New York, 1971.
[19] L. Robbiano, Théorème d'unicité adapté au contrôle des solutions des problèmes hyperboliques, *Comm. Partial Differential Equations* **16** (1991), no. 4–5, 789–800.
[20] A. Sharma, I. I. Rypina, R. Musgrave and G. Haller, Analytic reconstruction of a two-dimensional velocity field from an observed diffusive scalar, *J. Fluid Mech.* **871** (2019), 755–774.
[21] L. K. Su and W. J. A. Dahm, Scalar imaging velocimetry measurements of the velocity gradient tensor field in turbulent flows. I. Assessment of errors, *Phys. Fluids* **8** (1996), no. 7, 1869–1882.
[22] R. Temam, *Navier–Stokes Equations*, Stud. Math. Appl. 2, North-Holland, Amsterdam, 1979.
[23] C. Wunsch, Can a tracer field be inverted for velocity?, *J. Phys. Oceanography* **15** (1985), no. 11, 1521–1531.
[24] C. Wunsch, Using transient tracers: The regularization problem, *Tellus B* **39** (1987), no. 5, 477–492.